Nonlinear Dynamics of Reactive EEG Patterns under Cerebrovascular and Cardiovascular Distortions

Olga E. Dick

Pavlov Institute of Physiology of Russian Academy of Science, St. Petersburg, Russia
(E-mail: glazov.holo@mail.ioffe.ru)

Abstract. We examine the task of estimation of the differences in the human brain lability involving its opportunity to reproduce the external rhythm under cerebrovascular and cardiovascular distortions. For solving the task the electroencephalographic (EEG) patterns before, during and after intermittent photic stimulation are evaluated by the continuous wavelet transform and the recurrence quantification analysis. The degree of the human brain lability is estimated on the basis of changes in wavelet and recurrence features of the EEG patterns taking place under the photic stimulation. The coefficients of photic driving and holding and the energy increase times calculated by the wavelet spectra of the EEG patterns of patients with cerebrovascular and cardiovascular distortions differ significantly from the parameters determined for the healthy subjects. The study demonstrates the opportunity of nonlinear dynamics methods to estimate quantitatively the human brain lability of light stimulus perception for various groups of patients having cerebrovascular and cardiovascular distortions.
Keywords: EEG patterns, Wavelet transform, External rhythm, Multifractality, Cerebrovascular and Cardiovascular Pathologies

1 Introduction

As known, electroencephalography (EEG) time series reflects nonstationary dynamics of large neuron ensembles. The analysis of this dynamics is a possible tool for elucidating the degree of the brain seizures. However, sometimes evaluation of variations in EEG patterns is a rather complex problem as in distinguishing the diffuse neuronal activity arising as a late effect of cerebrovascular distortions from the normal one. To identify changes in the functional state clinicians use the functional probe as photic stimulation since sometimes variations in background EEG break down to reveal the changes [1]. Intermittent photic stimulation can induce a phenomenon of photic driving in EEG patterns, as a rule, time-locked to the light stimulus at a frequency identical to the frequency of light flashes [2]. Previously we have shown that parameters gained from wavelet spectra of reactive patterns for photic stimulation of patients with dyscirculatory encephalopathy differ significantly from the parameters of healthy subjects patterns [3]. The human healthy or sick brain demonstrates the different photic driving of beta, theta and alpha ranges and, therefore, the lability to reproduce or to reject the suggested rhythm in a different way.

Received: 21 April 2017 / Accepted: 26 October 2017

ISSN 2241-0503

The aim of the work is to estimate the parameters of the photic driving reaction for patients with cerebrovascular pathology in the form of vegetovascular dystonia and vertebrobasilar insufficiency and two types of cardiovascular pathology (persistent and paroxysmal atrial fibrillations).

2 Methods

2.1 EEG recording

The scalp EEG data were recorded from 10 healthy subjects and 12 patients with initial manifestations of cerebrovascular pathology in the form of vegetovascular dystonia, 14 patients having more severe symptoms in the result of vertebrobasilar insufficiency and 10 patients with cardiovascular pathology in the form of persistent atrial fibrillations and 11 patients with paroxysmal atrial fibrillations. The data were collected with electrodes placed at the occipital O1, O2, Oz sites. The recordings contained non- artifact segments in the three states: under resting condition, during photic stimulation and during relaxation between stimulations. The photostimulator was a xenon lamp with energy 0.3 J positioned in the dark room at a distance of 30 cm from the eyes. Intermittent photic stimulation was performed at 4, 6, 8, 10, 12 and 14 Hz. The stimulation lasted 9 seconds for each frequency, with a resting interval between frequencies of 30 seconds. The subjects kept their eyes closed throughout the experiment.

2.2. Estimation of the energy properties of the EEG pattern

To estimate the characteristics of EEG patterns and their variations taking place during the photic stimulation we apply the continuous wavelet transform:

$$W(a,t_0) = \frac{1}{a}\int_{-\infty}^{+\infty} x(t)\,\psi^*\left(\frac{t-t_0}{a}\right)dt,$$

where $x(t)$ is the examined EEG time series, $\psi((t- t_0)/a)$ is the wavelet function obtained from the basic wavelet $\psi(t)$ by scaling (stretching or compressing) and shifting along the time. The scale a determines the wavelet width and the space parameter t_0 gives the shift of the wavelet function along the time.

As the basic the complex Morlet wavelet is used:

$$\psi_0(t) = \pi^{-1/4}\exp(-0.5t^2)(\exp(i\omega_0 t) - \exp(-0.5\omega_0^2)),$$

where the second component in brackets can be neglected at $\omega_0=2\pi>0$. The value $\omega_0=2\pi$ gives the simple relation $f=1/a$ between the scale a and the frequency f of the Fourier spectrum. Then

$$W(f,t_0) = \pi^{-1/4}\sqrt{f}\int_{-\infty}^{+\infty} x(t)\exp(-0.5(t-t_0)^2 f^2)\exp(-i2\pi(t-t_0)f)dt.$$

The integral distribution of the wavelet spectrum energy over frequency range on the time interval $[t_1, t_2]$:

$$E(f)=\int_{t_1}^{t_2}\left|W(f,t_0)\right|^2 dt_0$$

describes the global wavelet spectrum and the integral distribution over time shifts t_0:

$$E(t_0)=\int_{f_C-\Delta f}^{f_C+\Delta f}\left|W(f,t_0)\right|^2 df$$

represents the fraction of the wavelet spectrum energy in the narrow range around the frequency f_C .

To compare the dynamics of two time series $x(t)$ and $y(t)$ and to evaluate the similarity of wavelet powers in both series one can use the wavelet cross spectrum:

$$\left|W_{xy}\right|=\left|W_x(f,t_0)W_y^*(f,t_0)\right|.$$

However, it can potentially lead to misleading results as it is just the product of two non-normalized wavelet spectrums [4]. The wavelet coherence (WC) avoids these mistakes by normalizing to the single wavelet power spectrum. The normalized value

$$WC=\frac{\left|S(W_{xy})\right|}{\sqrt{\left|S(W_{xx})\right|}\sqrt{\left|S(W_{yy})\right|}}$$

describes the wavelet coherence between two time series, where

$$\left|W_{xx}\right|=\left|W_x(f,t_0)W_x^*(f,t_0)\right|, \qquad \left|W_{yy}\right|=\left|W_y(f,t_0)W_y^*(f,t_0)\right|,$$

S denotes a smoothing operator used to balance between time-frequency resolution and statistical significance [4]. The value of WC ranges from 0 to 1 and describes local correlation between the two time series; the closer the value to 1, more the correlation between them. Statistically, significant wavelet coherences are identified using significance test [5]. A total of 100 realizations with the same first-order autoregressive (AR1) process coefficients as the two input data sets are generated using Monte Carlo techniques. The wavelet coherence is then calculated for each of these realizations and the significance level is calculated for each scale.

2.3 The light time series and estimation of photic driving

The light time series is approximated by a sequence of k Gauss impulses following each other with frequency f_C. The each impulse has the width r_O =10 ms. The centers of the impulses are in the points

$$t_j=t_A+j/f_c, \qquad \mathrm{j}=0,\ldots,k-1,$$

where t_A is the time of the light series switching, that is the time of the beginning of the first impulse in the sequence. Thus, the light stimulus is described by the function:

$$p(t) = \sum_{j=0}^{k-1} \frac{0.5}{r_0\sqrt{\pi}} \exp\left(-\frac{(t-t_j)^2}{4r_0^2} \right).$$

The frequency f_C is equal to 4, 6, 8, 10, 12 or 14 Hz.

The continuous wavelet transform of the signal $p(t)$ using the Morlet wavelet can be obtained in analytic form:

$$W_p(f,t_0) =$$

$$= \pi^{-1/4} \frac{\sqrt{f}}{\sqrt{g}} \sum_{j=0}^{k-1} \exp\left(-\left(\frac{f}{4r_0^2} + g \right)\left(t_j - t_0\right)^2 + i\frac{2\pi f^2}{g}\left(t_j - t_0\right) + \frac{(2\pi r_0)^2 f^3}{g} \right),$$

where the function $g = 1 + 2(r_0 f)^2$.

Fig.1 illustrates two examples of normalized integral distributions of wavelet spectra energies $e(t_0) = E(t_0)/E_{max}(t_0)$ of the EEG (dash-and-dot line) and light time series (solid red line). The integrals cross each other in two points (t_1, e_1) and (t_2, e_H) after switching on and switching off the light time series.

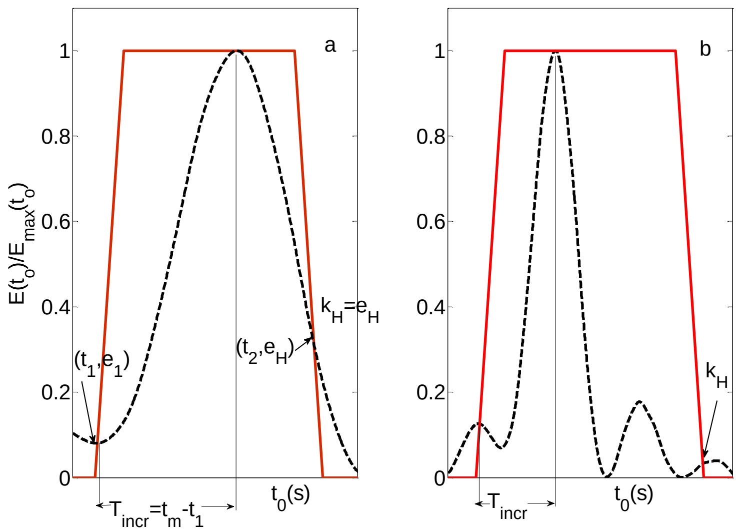

Fig.1 The normalized integral distributions of energies of wavelet spectra of the EEG (dash-and-dot line) and light time series (solid red line).

Let t_m be the moment of time when the normalized spectral integral of the EEG fragment reaches the maximal value. For the fraction of the wavelet spectrum energy between f_C - Δf and $f_C + \Delta f$ the energy increase time can be calculated as

$$T_{incr} = t_m - t_1.$$

This difference can characterize the time of remembering of the external rhythm since the smaller the value, the faster the photic driving [6]. In the first example (Fig. 1a) T_{incr} value is larger than in the second example (Fig. 1b) suggesting that remembering of the external rhythm is faster in the first case.

The normalized value e_H corresponding to the second point of intersection of two integral curves considered above can be taken as the coefficient of photic holding [6]:

$$k_H = e_H .$$

The smaller the value, the more badly the suggested rhythm of the photic stimulation is kept in the given fragment of EEG. In the second example (Fig. 1b) k_H is smaller testifying that in this case the external rhythm is held worse than in the first example.

The coefficient of photic driving (k_D) in the frequency range [f_C - Δf, $f_C + \Delta f$] can be determined by the ratio of the maxima of the global wavelet spectra during the photic stimulation ($E_{max}(f)_{during}$) with the frequency f_C and before it ($E_{max}(f)_{before}$) [6]:

$$k_D = E_{max}(f)_{during} / E_{max}(f)_{before}$$

The larger the value of k_D, the better the reproduction of the suggested external rhythm. If $k_D < 1$ then the energy of the global wavelet spectrum during the light stimulation is less than the energy in the resting state. It means the absence of the enhancement of the wavelet spectrum energy under exposure to the specific light time series.

2.4 The joint recurrence plot and estimation of photic driving

To evaluate photic driving reaction we also apply the recurrence quantification analysis [7] and the CRP Toolbox, available at *tocsy.pik-potsdam.de/crp.php*.
A joint recurrence plot (JRP) is a graphical representation of a matrix defined as

$$JR_{i,j}(m,\varepsilon) = \Theta\left(\varepsilon - \left\|x_i - x_j\right\|\right)\Theta\left(\varepsilon - \left\|y_i - y_j\right\|\right), i, j = 1,...,n,$$

where ε is an error (threshold distance for JRP computation), θ (·) is the Heaviside function, symbol || || denotes a norm, and x and y are phase space trajectories in a m-dimension phase space [7]. The trajectories are reconstructed from time series by using the delay coordinate embedding method [8].
The values $JR_{i,j} = 1$ and $JR_{i,j} = 0$ are plotted as gray and white dots, reflecting events that are termed as recurrence and nonrecurrence, respectively.

A recurrence will take place if a point x_j on the first trajectory returns to the neighbourhood of a former point x_i , and simultaneously a point y_j on the second trajectory returns to the neighbourhood of a former point y_i [7]. Thus, a JRP visualizes the simultaneous occurrence of recurrences in different time series (even physically different).

3. Results

The two time series (EEG patterns of the patient with cerebrovascular distortions in response of the photic stimulation of 14 Hz and the light stimulus) are shown in the left column of Fig.2. The light time series of 4 Hz and the corresponding EEG patterns of the patient with cardiovascular distortions are given in the right column of Fig.2.

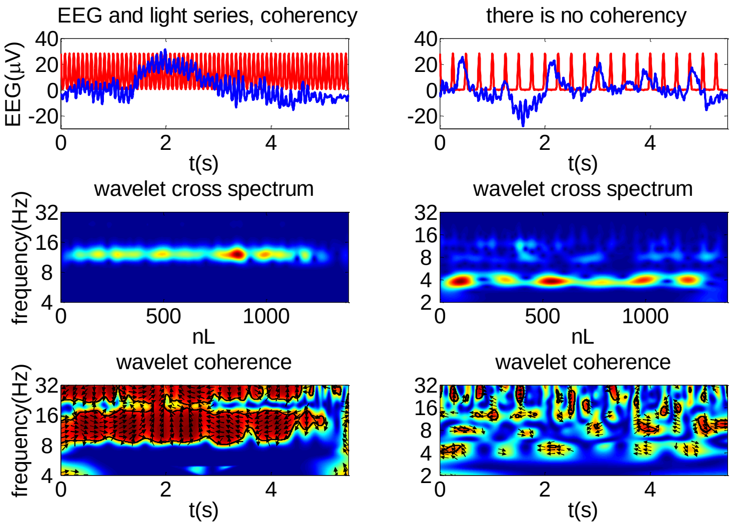

Fig.2 The light series of 14 Hz and 4 Hz (red lines) and the EEG during stimulation (blue curves) of two patients with cerebrovascular and cardiovascular distortions. The corresponding wavelet cross spectra and examples of wavelet coherence between the stimuli and responses. The color code for coherence ranges from blue (low coherence, close to zero) to red (high coherence, close to one).

The tight bands of the wavelet cross spectra in the both cases testify about local covariance between the light time series and the physiological response in the form of the EEG pattern. However, wavelet coherence analysis reveals large coherence between the stimulus and response only for the patient with cerebrovascular distortions (red regions during all the time of stimulation), suggesting the presence of mistakes in using the wavelet cross spectrum only[4].

The examples of the absence of the photic driving reaction at the frequency of 8 Hz and the presence of the weak photic driving reaction at the frequency of

10 Hz in the EEG patterns of the healthy subject are given in Fig. 3. The absence of the reaction is estimated by the absence of the enhancement of the global wavelet spectrum $E(f)$ around the stimulation (the blue curve as compared with the black one) and the absence of the increase of the integral distribution of the wavelet spectrum $E(t_0)/E_{max}(t_0)$ of the EEG pattern in response to the light time series. The presence the photic driving reaction is determined by the energy $E(f)$ enhancement around the stimulation frequency and the increase of the integral distribution $E(t_0)/E_{max}(t_0)$ in response to the light time series.

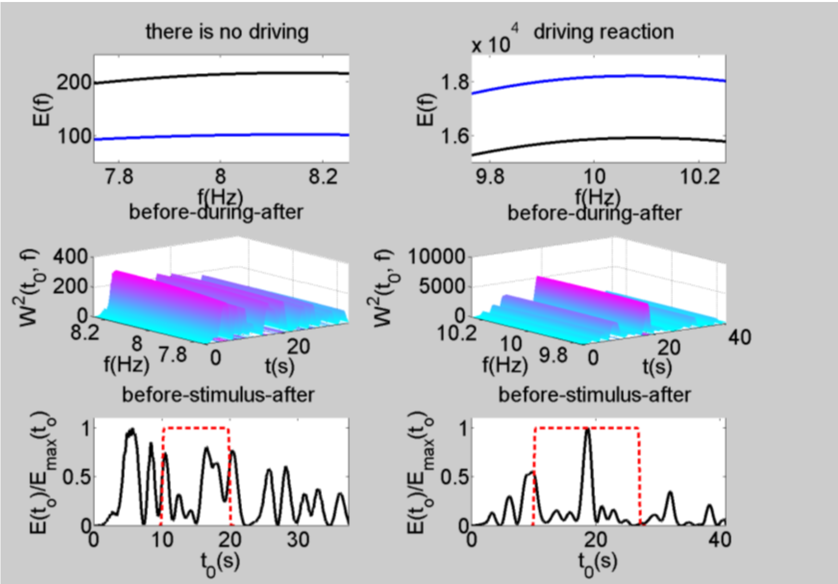

Fig.3 The absence of the photic driving reaction at the frequency of 8 Hz and the weak photic driving at the frequency of 10 Hz in the EEG patterns of the healthy subject. The wavelet surface $(t_0, f, |W(f, t_0)|^2)$ onto the (t_0, f) plane and the normalized integral distributions of energies of wavelet spectra of the EEG before, during and after stimulation (solid line) and the light time series (dash-and-dot red line).

The example of the photic driving reaction at the frequency of 8 Hz in the EEG fragment of the patient with vegetovascular dystonia is represented in Fig.4. The maximum of the wavelet surface is in the interval of the light stimulus action. One can see the slow enhancement of the wavelet energy and the large coefficient of photic holding of the suggested frequency.

Fig. 5 demonstrates also the slow enhancement of the wavelet energy and even more strong driving reaction to the frequency of 12 Hz for the patient with cardiovascular pathology in the form of paroxysmal atrial fibrillations.

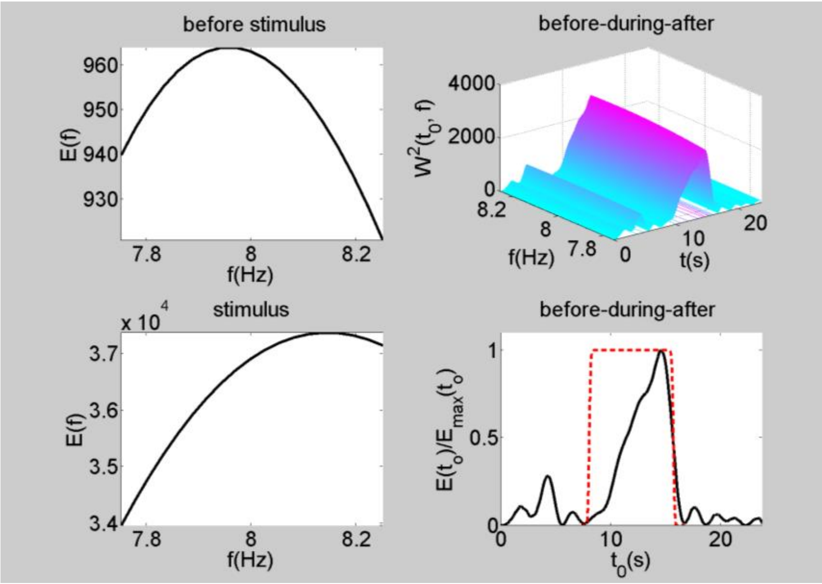

Fig.4. The slow enhancement of the wavelet energy and the large photic holding of the suggested rhythm in the EEG of the patient with vegetovascular dystonia.

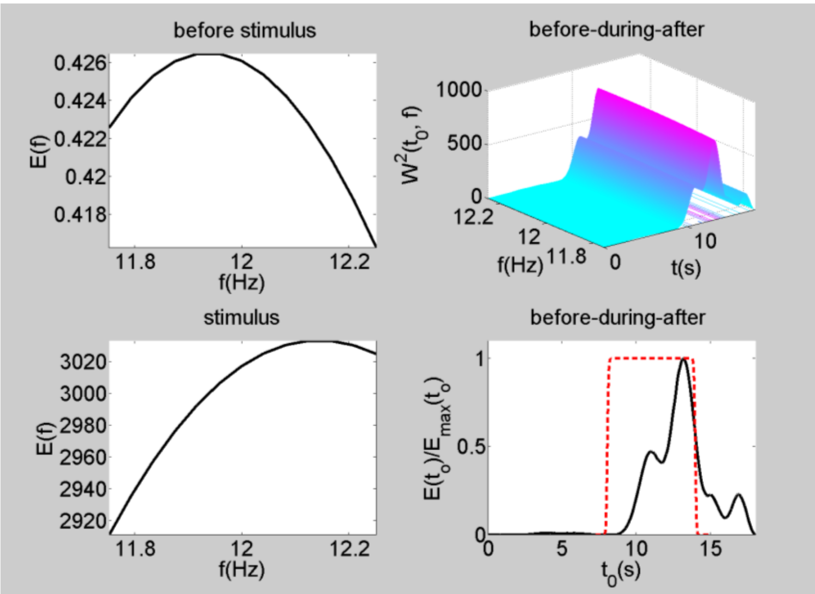

Fig.5. The slow enhancement of the wavelet energy and the large photic holding of the suggested rhythm in the EEG of the patient with paroxysmal atrial fibrillation.

The averaged (over the subjects in each group) values of the photic driving coefficient (k_D), the energy increase time (T_{incr}) during the photic stimulation and the photic holding coefficient (k_H) are given in Table 1. In all the frequency ranges the mean values of these coefficients significantly differ from the values obtained for the healthy subjects at the confidence level $p<0.05$ by the Mann-Whitney test. For the healthy persons the value $k_D < 1$ in all frequency intervals, that means the absence of the energy increase during the photic stimulation. A small enhancement above unit is evaluated only in the alpha range at the frequency of 10 Hz ($k_D = 1.31\pm0.06$), suggesting that the healthy subjects have only the weak photic driving in the alpha range.

In EEG patterns of the group with vegetovascular dystonia the photic driving reaction is observed in the theta, alpha and beta ranges. Frequencies of the beta range are reproduced faster and stronger than the other rhythms ($k_D = 120\pm4.7$, $T_{incr}=2.3\pm0.1$ s).

The patients with vertebrobasilar insufficiency reproduce the delta, theta, alpha and beta ranges but better of all they reproduce frequencies of the theta range since the photic driving coefficient as well as the photic holding coefficient have maximal values in this range ($k_D=1121\pm55$ and $k_H=0.88\pm0.05$, respectively). The energy increase time during the photic stimulation in the theta range is largest also ($T_{incr}=7.8\pm0.8$ s). Therefore, EEG patterns of this group of patients are characterized by the slow and strong driving of the theta rhythm.

For the patients with two types of cardiovascular pathology (persistent and paroxysmal atrial fibrillations) the photic driving reaction is noticed in the alpha range only. These groups differ by the values of the photic driving and holding coefficients. The patients with paroxysmal atrial fibrillations has slow strong driving of the alpha rhythm ($k_D=475\pm29$ and $k_H=0.51\pm0.03$) and patients with persistent atrial fibrillations has weak driving of this rhythm ($k_D=2.7\pm0.1$ and $k_H=0.25\pm0.01$).

state	rhythm	k_D	T_{incr}	k_H	driving
control	alpha	1.31±0.06	6.1±0.3	0.12±0.01	weak
vegetovas-cular dystonia	theta	20.1±1.5	3.1±0.1	0.45±0.02	fast strong driving of beta rhythm
	alpha	54.4±2.2	6.5±0.4	0.23±0.02	
	beta	120±4.7	2.3±0.1	0.21±0.02	
vertebro-basilar insufficiency	delta	30.4±1.8	6.3±0.4	0.81±0.04	slow strong driving of theta rhythm
	theta	1121±55	7.8±0.8	0.88±0.05	
	alpha	34.5±1.6	5.6±0.3	0.21±0.01	
	beta	54.5±2.2	5.2±0.3	0.11±0.006	
paroxysmal	alpha	475±29	3.2±0.1	0.51±0.03	strong
persistent	alpha	2.7±0.1	3.1±0.1	0.25±0.01	weak

Table 1 The mean values of the photic driving and holding coefficients (k_D and k_H) and the energy increase time (T_{incr}).

Thus, the patients with cerebrovascular distortions have the maximal reproduction of the external rhythm of the theta and beta ranges. The photic driving reaction terminates quickly for the patients with the vegetovascular dystonia and it continues longer for the patients with vertebrobasilar insufficiency. The reactive patterns of patients with cardiovascular distortions in the persistent form are similar to the control group. The reactive patterns of patients with paroxysmal fibrillations are characterized by the strong driving of the alpha rhythm.

Another evidence of the photic driving reaction in the EEG patterns is obtained with the joint recurrence plot analysis. Two EEG patterns during the photostimulation of the patients with paroxysmal and persistent atrial fibrillations and the light time series of 12 and 4 Hz as well as their joint recurrence plots are given in Fig. 6. The left JRP demonstrates the simultaneous occurrence of recurrences in the EEG pattern of the patient with paroxysmal atrial fibrillations and the light time series of 12 Hz whereas the right JRP is almost empty suggesting the absence of simultaneous recurrences of the EEG pattern of he patient with persistent type of fibrillations and the light time series of 4 Hz.

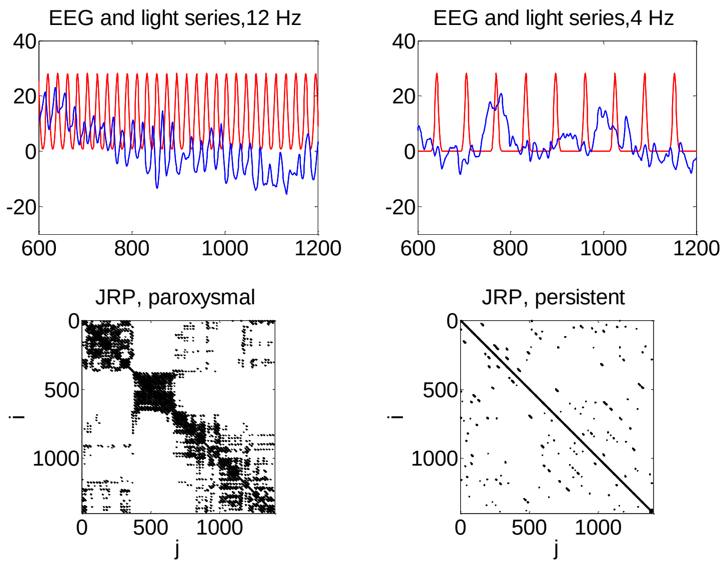

Fig. 6. Examples of the EEG patterns of the patients with paroxysmal and persistent atrial fibrillations during the photic stimulation and the joint recurrence plots of these patterns and light time series.
Parameters: the embedding dimension m=3, the delay time d =5, the threshold distance ε =1% of the standard deviation of the data series.

Conclusions

The absence of the photic driving reaction connected with the absence of the wavelet energy enhancement and the absence of simultaneous recurrences in the EEG patterns and the light time series are the characteristic features of the healthy subjects. The weak driving reaction in the alpha range is an exception to this rule. It reflects predominance of the internal synchronization of neuronal structures with driving the external rhythm for the healthy persons.

The presence of the photic driving reaction in the EEG patterns of the two examined groups of cerebrovascular pathology is likely due to the enhancement of instability of the internal synchronization. For the patients with vegetovascular dystonia the reproduction of the beta rhythm is more typical. It can be explained by the initiation of unstable neurodynamics due to the emergence of the pathological excitation focus in the central nervous system.

In EEG patterns of the patients with vertebrobasilar insufficiency this instability is amplified resulting in propagation of the pathological excitation focus and involvement of greater neuronal ensembles into pathological process. It leads to further disruption of the internal synchronization and growth of the external synchronization that accounts for greater increase of the energy characteristics and larger reproduction of the driving rhythm.

The weak photic driving reaction in the patterns of patients with cardiovascular pathology can be explained by the fall in excitability of the central nervous system due to vascular distortions of the brain as the result of chronic insufficiency of blood circulation.

References

1. J. M. E. Drake., K. E. Shy, L. Liss, Quantitation of photic driving in dementia with normal EEG. Clinical Electroencephalography, 20, 153{155, 1989.
2. I. Fedotchev, A. T. Bondar, I. G. Akoev, Dynamic characteristics of the human resonance EEG responses to rhythmic photostimulation. Human Physiology, 26, 64{72, 2000.
3. O.E. Dick, I. A. Svyatogor, Wavelet and multifractal estimation of the intermittent photic stimulation response in the electroencephalogram of patients with dyscirculatory encephalopathy. Neurocomputing, 165, 361{374, 2015.
4. D. Maraun, J. Kurths, Cross wavelet analysis: significance testing and pitfalls. Nonlinear Processes in Geophysics, 11, 505{514, 2004
5. A. Grinsted, J.C. Moore, S. Jevrejeva, S. Application of the cross wavelet transform and wavelet coherence to geophysical timeseries. Nonlinear processes in geophysics 11, 561{566, 2004.
6. O.E. Dick, Wavelet analysis of the human brain lability to reproduce the external rhythm. J. Chaotic Modeling and Simulation, 3, 387{394, 2013.
7. N. Marwan, M. C. Romano, M. Thiel, et. al. Recurrence plots for the analysis of complex systems. Physics Reports, 438, 237{329, 2007.
8. F. Takens. Detecting strange attractors in turbulence, Dynamical Systems and Turbulence, Lecture Notes in Mathematics (D. Rand, L. S. Young, eds.), Springer-Verlag, Berlin 898, 366{381, 1981